MOLECULAR AND CELLULAR BIOLOGY, Jan. 2002, p. 94–104 Vol. 22, No. 1
0270-7306/02/$04.00+0 DOI: 10.1128/MCB.22.1.94–104.2002
Copyright © 2002, American Society for Microbiology. All Rights Reserved.

Bcl-2 Family Members and Functional Electron Transport Chain Regulate Oxygen Deprivation-Induced Cell Death

David S. McClintock,[1] Matthew T. Santore,[1] Vivian Y. Lee,[1] Joslyn Brunelle,[1] G. R. Scott Budinger,[1] Wei-Xing Zong,[2] Craig B. Thompson,[2] Nissim Hay,[3] and Navdeep S. Chandel[1]*

Division of Pulmonary & Critical Care Medicine, Department of Medicine, Northwestern University Medical School,[1] and Department of Molecular Genetics, University of Illinois,[3] Chicago, Illinois, and Departments of Medicine and Pathology and Laboratory Medicine, Abramson Family Cancer Research Institute, University of Pennsylvania, Philadelphia, Pennsylvania[2]

Received 6 June 2001/Returned for modification 16 July 2001/Accepted 9 October 2001

The mechanisms underlying cell death during oxygen deprivation are unknown. We report here a model for oxygen deprivation-induced apoptosis. The death observed during oxygen deprivation involves a decrease in the mitochondrial membrane potential, followed by the release of cytochrome *c* and the activation of caspase-9. Bcl-X_L prevented oxygen deprivation-induced cell death by inhibiting the release of cytochrome *c* and caspase-9 activation. The ability of Bcl-X_L to prevent cell death was dependent on allowing the import of glycolytic ATP into the mitochondria to generate an inner mitochondrial membrane potential through the F_1F_0-ATP synthase. In contrast, although activated Akt has been shown to inhibit apoptosis induced by a variety of apoptotic stimuli, it did not prevent cell death during oxygen deprivation. In addition to Bcl-X_L, cells devoid of mitochondrial DNA (ρ° cells) that lack a functional electron transport chain were resistant to oxygen deprivation. Further, murine embryonic fibroblasts from *bax*$^{-/-}$ *bak*$^{-/-}$ mice did not die in response to oxygen deprivation. These data suggest that when subjected to oxygen deprivation, cells die as a result of an inability to maintain a mitochondrial membrane potential through the import of glycolytic ATP. Proapoptotic Bcl-2 family members and a functional electron transport chain are required to initiate cell death in response to oxygen deprivation.

Programmed cell death (apoptosis) plays an important role in the regulation of development morphogenesis, cell homeostasis, and diseases such as cancer, stroke, and ischemic heart disease (44, 49). Two pathways, the intrinsic and extrinsic pathways, by which cells can initiate and execute the cell death process have been identified (9, 42). The intrinsic apoptotic pathway is initiated within the cell by a loss of the outer mitochondrial integrity that leads to the redistribution of cytochrome *c* and other apoptotic regulatory proteins into the cytosol (9). Subsequently, cytochrome *c* in the cytoplasm interacts directly with Apaf-1, leading to the ATP-dependent formation of a macromolecular complex known as the apoptosome (26, 28). This complex recruits and activates the aspartyl-directed protease caspase-9. Activated caspase-9 can activate additional caspase-9 molecules, as well as caspase-3 and -7, resulting in the morphological features of apoptosis. If ATP is not available to form the apoptosome, then a necrotic form of cell death can occur (6). Antiapoptotic members such as Bcl-2 and Bcl-X_L prevent death that occurs through the intrinsic apoptotic pathway by preventing the loss of outer mitochondrial membrane integrity (21, 52). Proapoptotic Bcl-2 family members such as Bax and Bak are sufficient to initiate the loss of outer mitochondrial integrity, resulting in apoptosis (14, 22, 50). Moreover, either Bax or Bak is required for the execution of the intrinsic apoptotic pathway in response to serum deprivation or DNA-damaging agents such as etoposide and gamma irradiation (27, 51). Another regulator of the intrinsic pathway is phosphoinositide-3 kinase (PI3K) and its downstream target Akt. An activated form of Akt can confer cell survival in the absence of growth factors and inhibits apoptosis induced by a wide range of stimuli (4, 15).

The extrinsic apoptotic pathway begins when a death ligand, such as FasL, interacts with its cell surface receptor, Fas, and initiates the formation of a death-inducing signaling complex that recruits and activates caspase-8 (33). In this pathway, strong activation of caspase-8 directly activates caspase-3, resulting in apoptosis. In some cell types, caspase-8 activation is insufficient to activate caspase-3 alone. In these cells, caspase-8 activation is amplified through the mitochondria (35). This process occurs by the initiation of caspase-8-dependent cleavage of Bid, a proapoptotic factor. A truncated Bid induces the loss of outer mitochondrial membrane integrity, leading to cytochrome *c* release and caspase-9 and caspase-3 activation (25, 30).

Although much progress has been made in uncovering pathways and factors involved in apoptosis in response to loss of survival signals, DNA-damaging agents, and the activation of death receptors, little is known about the mechanisms underlying cell death in response to oxygen deprivation. Several studies have suggested that cells die through apoptosis in response to oxygen deprivation (16, 39). Moreover, studies have demonstrated that antiapoptotic members of the Bcl-2 family and the 150 kDa oxygen-regulated protein prevent cell death during oxygen deprivation (17, 41, 43). The translocation of the proapoptotic Bcl-2 family member Bax from the cytosol to mitochondria has also been observed during oxygen depriva-

---

* Corresponding author. Mailing address: Division of Pulmonary & Critical Care Medicine, Department of Medicine, Northwestern University Medical School, Chicago, IL 60601-3010. Phone: (312) 908-8163. Fax: (312) 908-4650. E-mail: nav@northwestern.edu.

tion (38). The aim of the present study was to examine how oxygen deprivation initiates cell death and the role of Bcl-2 family members in regulating oxygen deprivation-induced cell death.

MATERIALS AND METHODS

Cell culture. Rat1a fibroblasts, HT1080 fibrosarcoma cells, and murine embryonic fibroblasts (MEFs) were cultured at 30 to 50% confluence in Dulbecco's modified essential medium supplemented with HEPES (10 mM), pyruvate (1 mM), penicillin (100 U/ml), streptomycin (100 μg/ml), and 10% heat-inactivated fetal bovine serum (Gibco). Rat1a fibroblasts containing a Src myristoylation signal fused to the c-Akt coding sequence (Myr-Akt) and the control puromycin vector (Puro) or overexpressing Bcl-X_L and the control neomycin vector (Neo) were generated as previously described (7). Wild-type HT1080 cells were incubated in Dulbecco's modified essential medium containing ethidium bromide (100 ng/ml), sodium pyruvate (1 mM), HEPES (10 mM), and uridine (100 μg/ml) to generate HT1080 cells devoid of mitochondrial DNA (ρ° cells). MEFs were generated from wild-type, *p53*$^{-/-}$, or *bax*$^{-/-}$ *bak*$^{-/-}$ embryos. HT1080 cells transfected with the control vector or manganese superoxide dismutase (MnSOD) and catalase targeted to the mitochondria were gifts from Andres Melendez (37). Oxygen deprivation conditions (0% O_2, 85% N_2, 10% H_2, and 5% CO_2) were achieved in a humidified anaerobic workstation at 37°C (BugBox; Ruskinn Technologies). An anaerobic color indicator (Oxoid Limited) confirmed anaerobicity of the chamber. Hypoxic conditions (1.5% O_2, 93.5% N_2, and 5% CO_2) were achieved in a humidified variable aerobic workstation (Invivo O_2; Ruskinn Technologies). The Invivo O_2 contains an oxygen sensor that continuously monitors the chamber oxygen tension. The caspase inhibitor *N*-benzyloxycarbonyl-Val-Ala-Asp-fluoromethyl-ketone (zVAD-fmk; Enzyme Systems Products) was administered at a concentration of 100 μM, 1 h prior to incubation of cells under oxygen deprivation conditions.

Measurement of cell death. Cell death was assayed by measuring lactate dehydrogenase activity (LDH) in culture supernatants from cells plated on 60-mm culture plates with a cytotoxicity detection kit (Roche Molecular Biochemicals) according to the manufacturer's protocol. Apoptosis was detected either by determining the percentage of cells that had condensed and fragmented nuclei by staining with Hoechst no. 33258 (1 μg/ml; Sigma) as previously described (2) or by measuring cytoplasmic histone-associated-DNA fragments following cell death with the cell death detection ELISA^{Plus} kit (Roche Molecular Biochemicals) according to the manufacturer's protocol.

Western blot analysis for cytochrome *c* release. Cytosolic fractions were prepared by scraping cells in ice cold buffer (250 mM sucrose, 20 mM HEPES, 10 mM KCl, 1.5 mM $MgCl_2$, 1 mM EDTA, 1 mM EGTA, 1 mM dithiothreitol). Cells were homogenized with a cylinder cell homogenizer for 20 s, and unlysed cells and nuclei were collected by centrifugation at 800 × *g* for 10 min. The supernatant was collected and spun at 22,000 × *g* for 15 min to separate the cytosolic and mitochondrial fractions. The resulting cytosolic fraction was collected, and the proteins in the samples were quantified by the Bio-Rad protein assay. Cytosolic or mitochondrial fractions (100 μg) were mixed with an equal volume of sample loading buffer (125 mM Tris base [pH 6.8], 4% [wt/vol] sodium dodecyl sulfate, 20% (vol/vol) glycerol, 200 mM dithiothreitol, 0.02% [wt/vol] bromphenol blue). After heating, the protein was resolved on a sodium dodecyl sulfate–15% polyacrylamide gel and transferred to a Hybond-ECL nitrocellulose membrane (Amersham). After transfer, the gel was stained with Ponceau S to verify uniform loading and transfer. Membranes were blocked with 5% (wt/vol) nonfat milk in TBS-T (100 mM Tris base [pH 7.5], 0.9% [wt/vol] NaCl, 0.1% [vol/vol] Tween 20) overnight and subsequently incubated with 1 μg of the 7H8.2C12 anti-cytochrome *c* antibody (Pharmingen) per ml or with 0.5 μg of 20E8-C12 anti-cytochrome *c* oxidase subunit IV antibody (Molecular Probes) per ml overnight at 4°C. The membrane was washed with TBS-T three times and incubated for 1.5 h at room temperature with horseradish peroxidase-conjugated secondary antibody (Amersham). The membrane was washed three times with TBS-T and analyzed by enhanced chemiluminescence (Amersham).

Measurement of caspase activity. Caspase-9 and caspase-8 enzymatic activity was measured with fluorometric assay kits specific to each caspase (R&D Systems). Cell were plated onto 100-mm culture dishes at 40 to 60% confluence, and caspase activity was measured according to the manufacturer's protocol using a fluorescent microplate reader. Data were normalized to total protein concentration as determined by the Bio-Rad protein assay.

Measurement of ATP levels. ATP levels were measured by the luciferin-luciferase method using an ATP bioluminescence assay kit (HS II; Roche Molecular Biochemicals). Cells were lysed with lysis buffer provided by the manufacturer. Luciferase reagent (50 μl) was manually injected into 50 μl of cell lysate, and luminescence was analyzed after a 30-s delay with a 2-s integration on a SpectraMax Gemini microplate reader (Molecular Devices). A standard curve was generated from known concentrations of ATP and used to calculate the concentration of ATP in each sample. Luminescence increased linearly with the negative log of the ATP concentration in the samples over the range of concentrations measured. Data were normalized to total protein concentration as determined by the Bio-Rad protein assay.

Measurement of Ψ. To assess the change in mitochondrial membrane potential (Δψ) in cells exposed to oxygen deprivation, cells were plated onto 60-mm culture dishes at 40 to 60% confluence and incubated for 1 h in the presence of two fluorescent probes, tetramethylrhodamine ethyl ester (TMRE; excitation, 550 nm; emission, 580 nm; 500 nM) and Mitotracker green (MITO; excitation, 490 nm; emission, 515 nm; 2 μM) (Molecular Probes). Cells were lysed with 1% (vol/vol) Triton X-100, and fluorescence was measured on a SpectraMax Gemini microplate reader (Molecular Devices). TMRE localizes within mitochondria, and its fluorescence increases in proportion to ψ. As ψ diminishes, so does TMRE fluorescence. MITO localizes to mitochondria independently of Δψ and reflects the number of mitochondria within a given cell. The ratio between TMRE fluorescence and MITO fluorescence reflects ψ normalized to the number of mitochondria. As a control for each condition, cells were incubated with both TMRE and MITO in the presence of the protonophore carbonyl cyanide trifluoromethoxyphenylhydrazone (FCCP, 20 μM; Sigma), which dissipates the ψ. The TMRE/MITO ratio for each condition was subtracted from the TMRE/MITO ratio in the presence of FCCP.

Measurement of VEGF levels. Vascular endothelial growth factor (VEGF) levels were measured in culture supernatants from cells plated on 60-mm culture dishes with a mouse VEGF Quantikine M immunoassay kit (R&D Systems) according to the manufacturer's protocol. Data were normalized by using total protein concentration as determined by the Bio-Rad protein assay.

Statistical analysis. The data presented are means ± standard errors of the means of four independent experiments unless otherwise stated. Data were analyzed by one-way analysis of variance. When the analysis of variance indicated a significant difference, individual differences were explored with Student's *t* test by using the Bonferroni correction for multiple comparisons. Statistical significance was determined at the 0.05 level.

RESULTS

Bcl-X_L prevents cell death due to oxygen but not oxygen and glucose deprivation. Rat1a fibroblasts transfected with a control vector (Neo) or Bcl-X_L were incubated in an environment deprived of oxygen for 24 and 48 h, and cell death was determined by the release of LDH. Neo control cells exhibited an increase in cell death upon oxygen deprivation, whereas Bcl-X_L cells did not (Fig. 1A). In order to determine whether the cell death observed during oxygen deprivation was apoptotic, control and Bcl-X_L cells were examined for cytoplasmic histone-associated DNA fragments following a 24-h exposure to 21 or 0% O_2 (Fig. 1B). Neo control cells displayed an approximately 2.5-fold increase in DNA fragmentation over basal levels, whereas Bcl-X_L cells did not show a significant increase. These data demonstrate that Bcl-X_L protects cells from oxygen deprivation-induced apoptosis.

Conditions in which cells are deprived of oxygen are often accompanied by lack of glucose. Therefore, Neo control and Bcl-X_L cells were incubated in media deprived of both oxygen and glucose, supplemented with 12 mM 2-deoxyglucose (2-DOG), for 8 and 12 h and assayed for LDH release (Fig. 1C). Unlike in oxygen deprivation alone, Bcl-X_L did not prevent cell death under these conditions. Following 12 h of oxygen and glucose deprivation, however, there was not a significant increase in DNA fragmentation in either the Neo control or Bcl-X_L cells (Fig. 1D). These observations were confirmed by examining condensed and fragmented nuclei with Hoechst staining in fixed Neo and Bcl-X_L cells exposed to 0% O_2 with or without 2-DOG. Neo control cells under 0% O_2 alone

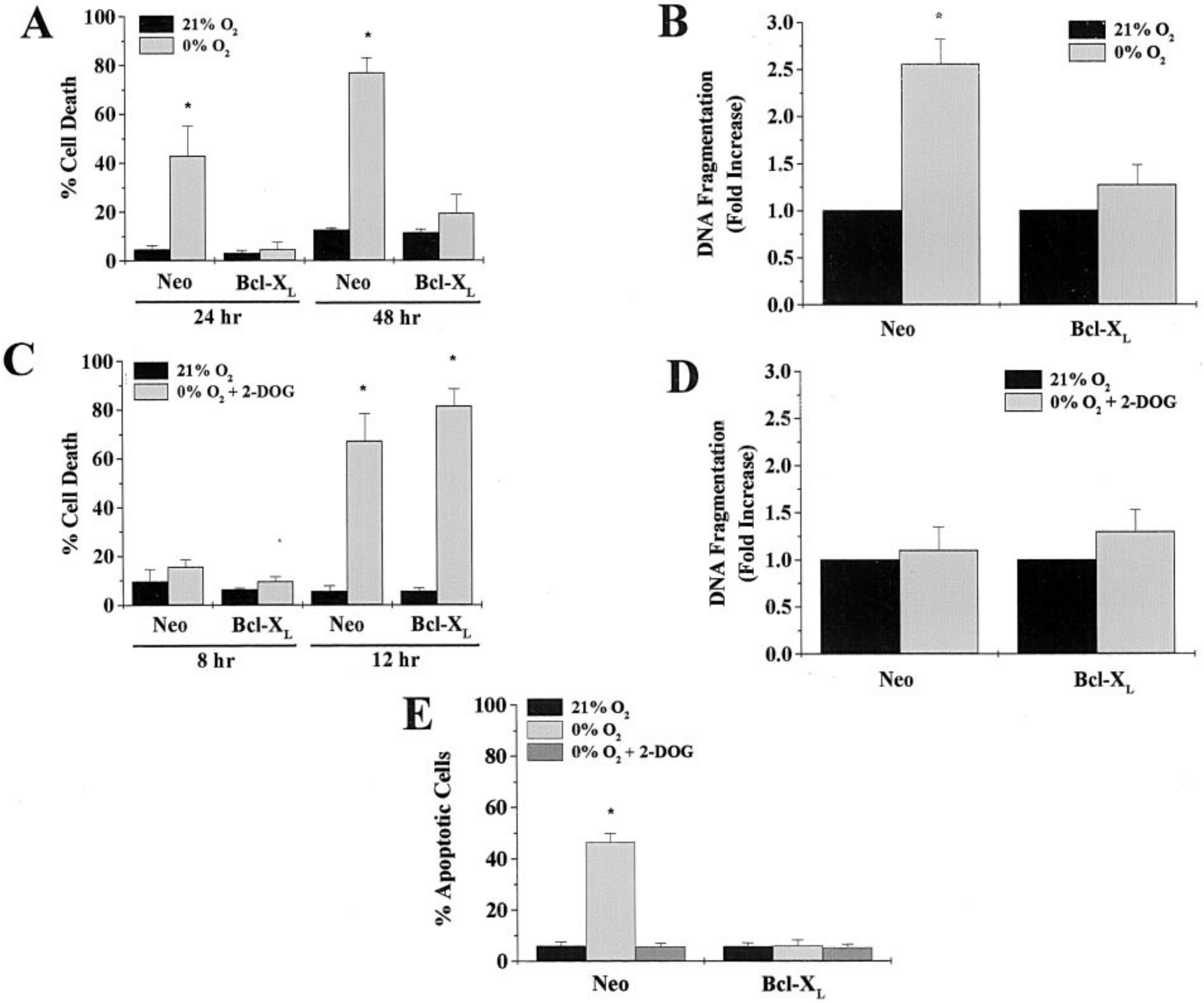

FIG. 1. Bcl-X_L prevents cell death in response to oxygen deprivation but not oxygen and glucose deprivation. (A) Rat1a fibroblasts stably transfected with a control vector (Neo) or Bcl-X_L were exposed to 0% O_2 for 24 and 48 h and assayed for LDH release, as described in Materials and Methods. (B) Neo control and Bcl-X_L cells were exposed to 0% O_2 for 24 h and assayed for cytoplasmic histone-associated-DNA fragments. (C) Neo control and Bcl-X_L cells in glucose-free media supplemented with 12 mM 2-DOG were exposed to 0% O_2 for 8 and 12 h and assayed for LDH release. (D) Neo control and Bcl-X_L cells in glucose-free media supplemented with 2-DOG (12 mM) were exposed to 0% O_2 for 12 h and assayed for cytoplasmic histone-associated-DNA fragments. (E) Percentage of apoptotic cells scored by Hoechst staining of Neo control and Bcl-X_L cells exposed to 0% O_2 with or without 2-DOG (12 mM) for 24 h. *, $P < 0.05$ compared with Neo control cells exposed to 21% O_2.

displayed apoptotic nuclei, whereas Bcl-X_L cells under 0% O_2 did not. Neither Neo nor Bcl-X_L cells displayed apoptotic nuclei when exposed to 0% O_2 plus 2-DOG (Fig. 1E). These data demonstrate that Bcl-X_L does not prevent necrotic cell death from oxygen deprivation when glucose availability is limited.

Commitment to cell death during oxygen deprivation occurs at the point of cytochrome *c* release. Rat1a fibroblasts incubated for 8 and 16 h with 0% oxygen did not display a cell death rate above normoxic control levels. Only after 24 h of oxygen deprivation did cell death increase significantly (Fig. 2A). To test how long cells could survive oxygen deprivation before committing to apoptosis, Rat1a fibroblasts were exposed to oxygen deprivation for various intervals and subsequently returned to normal oxygen levels. Rat1a fibroblasts exposed to 0% O_2 for 8 h and 21% O_2 for 16 h did not show an increase in cell death, whereas cells exposed to 0% O_2 for 16 h and 21% O_2 for 8 h showed a rate of cell death similar to that seen in cells exposed to 0% O_2 for 24 h (Fig. 2B). These data suggest that the commitment to death occurs between 8 and 16 h of oxygen deprivation.

To examine whether the commitment to death was at the point of cytochrome *c* release, Neo control and Bcl-X_L cells were exposed to 0, 8, or 16 h of 0% O_2 and to 8 h of simultaneous glucose and oxygen deprivation. Subcellular fractions were prepared, and the cytosolic fraction was analyzed for cytochrome *c* content by immunoblotting (Fig. 2C). Consistent with Fig. 2B, cytochrome *c* did not accumulate in the cytosol until after 16 h of oxygen deprivation in the control cells. Bcl-X_L cells did not show an accumulation of cytochrome *c* in the cytosolic fraction under oxygen deprivation. However, both the control and Bcl-X_L cells did show an accumulation of

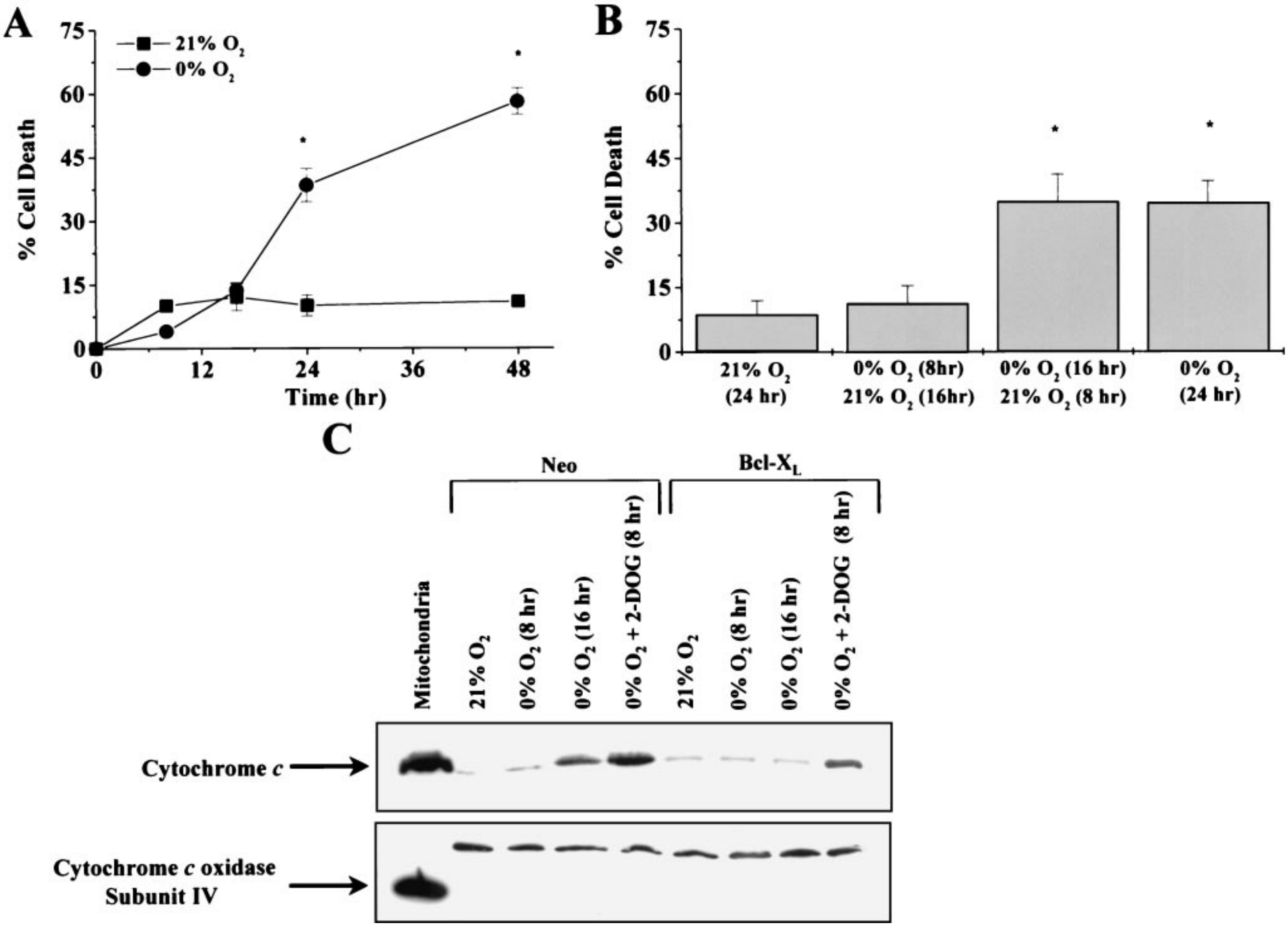

FIG. 2. Cells exposed to oxygen deprivation commit to death at the point of cytochrome *c* release. (A) Rat1a fibroblasts were exposed to 0% O_2 for 8, 16, 24, and 48 h and assayed for LDH release. (B) Rat1a cells were exposed to 0% O_2 for 8 and 16 h and then reintroduced into 21% O_2 for 16 and 8 h, respectively, and assayed for LDH release. *, $P < 0.05$ compared with cells exposed to 21% O_2. (C) Cytosolic fractions probed with either cytochrome *c* or cytochrome *c* oxidase subunit IV following 8 and 16 h of oxygen deprivation (0% O_2) or 8 h of oxygen and glucose deprivation (0% O_2 + 2-DOG) in Neo and Bcl-X_L cells. The mitochondrial fraction was included as a control.

cytochrome *c* when exposed to oxygen and glucose deprivation. The irreversible broad-range caspase inhibitor zVAD-fmk (100 μM) did not prevent the release of cytochrome *c* (data not shown), indicating that oxygen deprivation-induced release of cytochrome *c* was not dependent on caspase activation.

Caspase-9 is activated during oxygen deprivation. Cytochrome *c*, following release from the mitochondria, has been shown to bind to apoptotic protease activating factor (Apaf-1), which then undergoes a conformational change that allows the cleavage and activation of caspase-9 (26, 28). This process requires ATP. The activated form of caspase-9 subsequently triggers a caspase cascade that results in cell death. To test whether the release of cytochrome *c* during oxygen deprivation led to the activation of caspase-9, Neo control and Bcl-X_L-expressing cells were exposed to 0% O_2 for 8 and 16 h, and caspase-9 activity was measured. Neo control cells exhibited a significant increase in caspase-9 activity after 16 h of oxygen deprivation (Fig. 3A). Bcl-X_L-expressing cells did not show an increase in caspase-9 activity during oxygen deprivation. Caspase-8 activity in control and Bcl-X_L-transfected cells was also examined following 8- and 16-h exposures to 0% O_2, but no significant increases in activity were found (data not shown).

Control and Bcl-X_L cells exposed to 8 h of oxygen and glucose deprivation did not display an increase in caspase-9 activity (Fig. 3A). Because cells deprived of both oxygen and glucose exhibited release of cytochrome *c* but not activation of caspase-9 (Fig. 2C), we examined ATP levels. Both control and Bcl-X_L cells had decreased ATP levels over a 16-h period during oxygen deprivation compared to normal oxygen conditions (Fig. 3B). When control and Bcl-X_L-transfected cells were subjected to oxygen and glucose deprivation for 8 h, their ATP dropped to undetectable levels (data not shown).

Akt does not prevent oxygen deprivation-induced cell death. The phosphoinositide-3 kinase–Akt pathway is a potent mediator of cell survival signals (4). This pathway also has been shown to mediate the release of factors that initiate the formation of new blood vessels (angiogenesis) (13, 32). Cells that are beginning to be deprived of oxygen ($[O_2] < 3\%$) stimulate the release of angiogenic factors such as VEGF. This adaptive response is to prevent states of a complete absence of oxygen and nutrients. We examined the ability of activated Akt both to

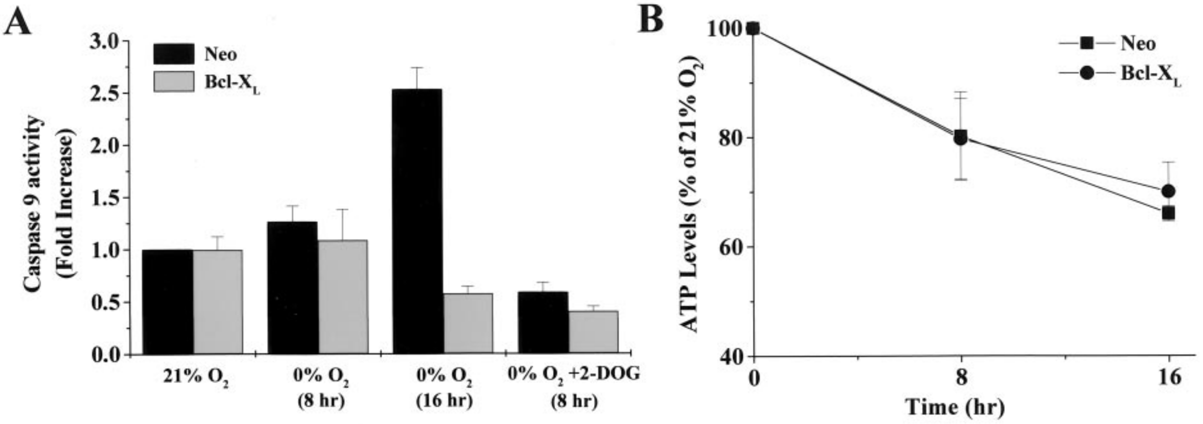

FIG. 3. Caspase-9 is activated during oxygen deprivation. (A) Neo control and Bcl-X$_L$-transfected cells were exposed to 0% O$_2$ for 8 and 16 h or 0% O$_2$ plus 2-DOG for 8 h and assayed for caspase-9 activity. Data are normalized to the Neo control cells at 21% O$_2$. (B) Neo control and Bcl-X$_L$ cells were exposed to 0% O$_2$ for 0, 8, and 16 h, and the levels of ATP were measured and standardized for ATP content at 0 h.

confer a signal that prevents oxygen deprivation-induced cell death and to stimulate VEGF levels under normal oxygen conditions. Rat1a fibroblasts stably expressing an activated form of Akt (Myr-Akt) consisting of the Src myristoylation signal fused to the c-Akt coding sequence were exposed to 24 and 48 h of 0% O$_2$ and then assayed for LDH release. After 48 h of oxygen deprivation, the control transfected cells (Puro) and Myr-Akt cells showed similar significant increases in cell death rates over those at normal oxygen levels (Fig. 4A). Akt, unlike Bcl-X$_L$, is not able to rescue cells from death by oxygen deprivation. Similar results have recently been observed for glucose deprivation (7, 36). However, Myr-Akt cells did display an increase in the angiogenic factor VEGF under normal and hypoxic (1.5% O$_2$) conditions (Fig. 4B). Collectively, these results indicate that Akt does not intrinsically prevent cell death during oxygen deprivation but stimulates the release of angiogenic factors that would help prevent states of oxygen deprivation.

Oxygen deprivation-induced cell death requires a functional electron transport chain and is dependent upon Bax or Bak. To further elucidate the role of the mitochondria during oxygen deprivation-induced cell death, HT1080 human fibrosarcoma cells lacking a functional mitochondrial electron transport chain (ρ° cells) were exposed to 0% O$_2$ or doxorubicin (0.25 μg/ml) for 48 h and assayed for LDH release. The wild-type HT1080 cells displayed an increase in cell death under oxygen deprivation. In contrast, the ρ° HT1080 cells did not show a significant increase in cell death (Fig. 5A). The ρ° HT1080 cells were still sensitive to doxorubicin, indicating that the death machinery was functional in these ρ° cells. Thus, functional electron transport is required for oxygen deprivation-induced cell death.

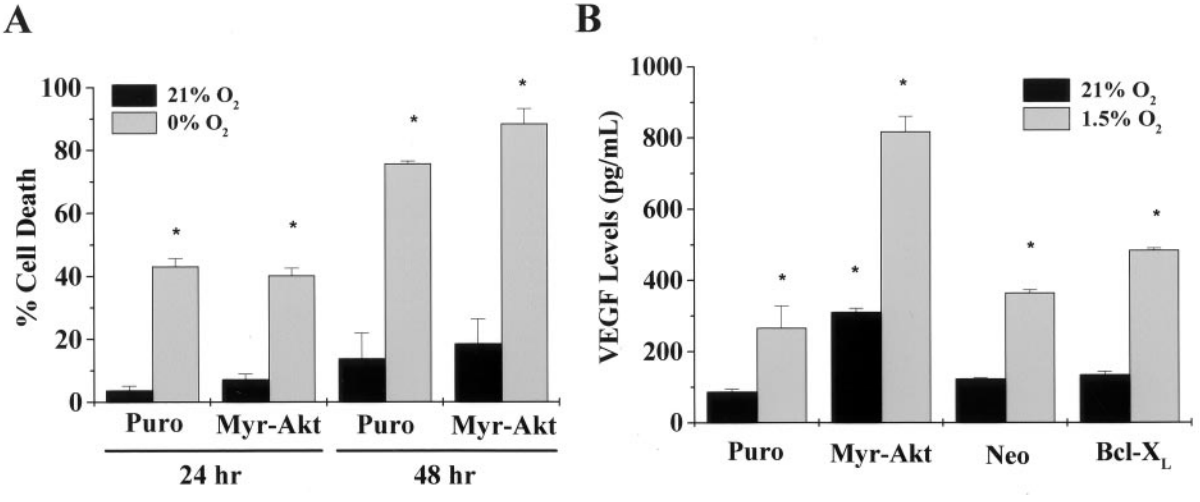

FIG. 4. Akt does not prevent oxygen deprivation-induced cell death. (A) Rat1a cells stably transfected with a control vector (Puro) or Src myristoylated Akt (Myr-Akt) were exposed to 0% O$_2$ for 24 and 48 h and assayed for LDH release. *, $P < 0.05$ compared with Puro control cells exposed to 21% O$_2$. (B) Control, Myr-Akt, and Bcl-X$_L$-transfected cells were exposed to 21 and 1.5% O$_2$ for 24 h and assayed for VEGF release into the culture supernatant. *, $P < 0.05$ compared with Puro or Neo control cells exposed to 21% O$_2$.

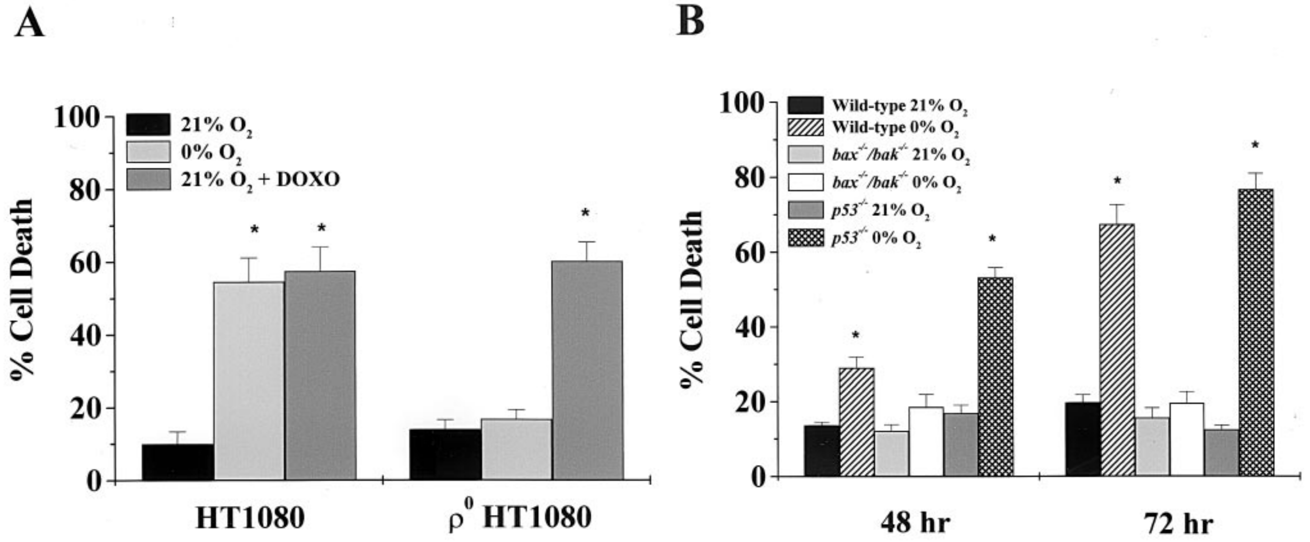

FIG. 5. Oxygen deprivation-induced cell death requires functional electron transport and is dependent upon Bax or Bak. (A) Wild-type and ρ° HT1080 human fibrosarcoma cells were exposed to 0% O_2 or doxorubicin (DOXO, 0.25 μg/ml) for 48 h and assayed for LDH release. (B) Wild-type, $bax^{-/-}$ $bak^{-/-}$, and $p53^{-/-}$ MEFs were exposed to 0% O_2 for 48 and 72 h and assayed for LDH release. The data are the means and standard errors of the means of six independent experiments. *, $P < 0.05$ compared with wild-type cells exposed to 21% O_2.

DNA-damaging agents and serum deprivation-induced cell death require Bax or Bak (51). To determine the role of p53 and Bax or Bak in oxygen deprivation-induced cell death, MEFs from wild-type, $bax^{-/-}$ $bak^{-/-}$, or $p53^{-/-}$ mice were deprived of oxygen for 48 and 72 h and assayed for LDH release. $p53^{-/-}$ MEFs were sensitive to oxygen deprivation (Fig. 5B). In contrast, $bax^{-/-}$ $bak^{-/-}$ MEFs were resistant to oxygen deprivation (Fig. 5B). These results indicate that oxygen deprivation-induced cell death is independent of p53 but requires Bax or Bak.

Oxygen deprivation-induced cell death occurs independently of the mitochondrial PTP or ROS. The permeability transition pore (PTP) has been implicated as a possible mechanism of mitochondrial release of cytochrome *c* under conditions of oxygen deprivation (24). Oxidative stress has been shown to contribute to conditions that favor PTP formation. Reactive oxygen species (ROS) can be generated under virtually anaerobic conditions (5). To test whether the involvement of the mitochondrial PTP was required during oxygen deprivation-induced cell death, Rat1a fibroblasts were pretreated with PTP inhibitors cyclosporine or trifluoperazine (TPZ), exposed to 0% O_2 for 48 h, and assayed for LDH release. Cyclosporine and TPZ did not prevent oxygen deprivation-induced cell death (Fig. 6A). However, cyclosporine did prevent cell death induced by thapsigargin, a selective inhibitor of the endoplasmic reticulum-associated calcium ATPase, in the presence of hydrogen peroxide (Fig. 6B). To test the role of ROS during oxygen deprivation-induced cell death, Rat1a fibroblasts were incubated with Mn(III)tetrakis (4-benzoic acid) porphyrin (MnTBAP), a superoxide scavenger, and *N*-acetylcysteine (NAC), a hydrogen peroxide scavenger, for 1 h under normal oxygen conditions and subsequently exposed to 0% O_2 for 48 h. MnTBAP and NAC did not prevent LDH release, suggesting that antioxidants do not prevent cell death during oxygen deprivation (Fig. 6C). We further assessed the role of ROS by exposing HT1080 fibrosarcoma cells transfected with MnSOD and catalase targeted to the mitochondria to 0% O_2 for 48 h. These cells exhibit a 13.2-fold increase in catalase activity and a 15.0-fold increase in MnSOD activity (37). However, the overexpression of MnSOD and catalase targeted to the mitochondria did not prevent cell death under oxygen deprivation conditions (Fig. 6D). Collectively, these results suggest that oxygen deprivation-induced cell death does not depend on either the mitochondrial PTP or the generation of ROS.

Bcl-X_L prevents cell death by allowing glycolytic ATP to maintain a partial ψ via the F_1F_0-ATP synthase. During anaerobic conditions electron transport chain ceases, resulting in the depolarization of the inner mitochondrial membrane. Previous studies have shown that early events in the commitment of cells to release cytochrome *c* are changes in mitochondrial membrane potential (ψ) (47). Bcl-X_L prevents the change in ψ and subsequent apoptosis. We examined changes in ψ in Neo control and Bcl-X_L-transfected Rat1a fibroblasts exposed to 0% O_2 for 8, 16, and 24 h. ψ was measured using the ratio of TMRE and MITO. TMRE fluorescence is dependent on ψ, while MITO fluorescence is independent of $\Delta\psi$ and reflects the number of mitochondria within a given cell. Neo control Rat1a fibroblasts exhibited 41.52% ± 8.00% and 83.15% ± 6.79% decreases in ψ at 8 and 16 h, respectively, after being exposed to 0% O_2 (Fig. 7A). Because cytochrome *c* release was observed only at 16 h, these results suggest that depolarization of the inner mitochondrial membrane precedes the release of cytochrome *c*. Moreover, zVAD-fmk did not prevent the decrease in ψ, suggesting that caspases are not responsible for the loss of ψ during oxygen deprivation (data not shown). Cells expressing Bcl-X_L maintained a partial potential (~50%) over the 48 h period. The ability of Bcl-X_L to maintain a ψ without a functional electron transport chain led us to examine whether ATP generated by glycolysis was being imported into mito-

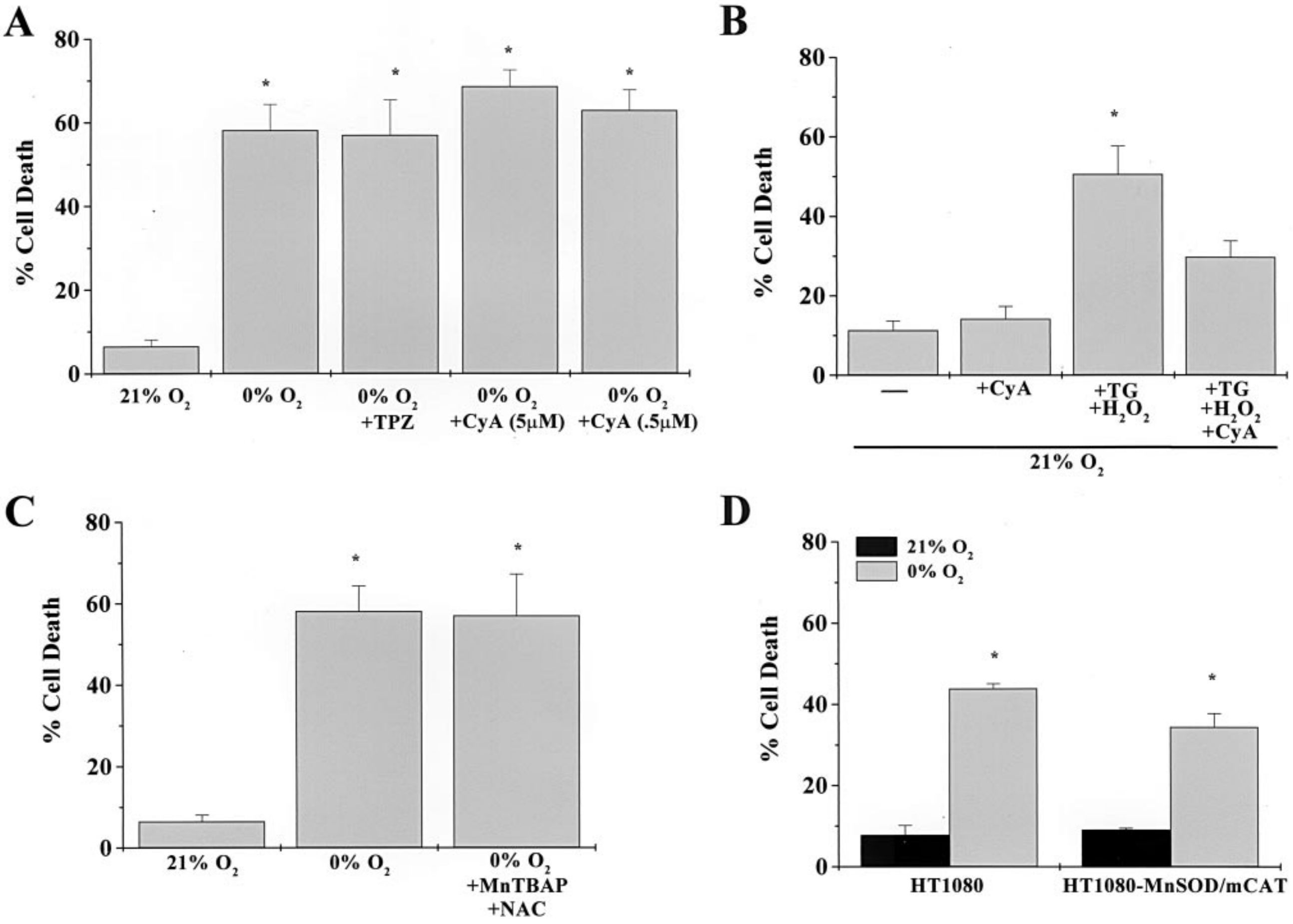

FIG. 6. Oxygen deprivation-induced cell death occurs independently of the mitochondrial PTP or ROS. Cell death was assayed by LDH release. (A) Rat1a fibroblasts were pretreated with the PTP inhibitors cyclosporine (CyA, 0.5 or 5 μM) and TPZ (5 μM) for 1 h, followed by exposure to 0% O_2 for 48 h. (B) Rat1a fibroblasts were pretreated with cyclosporine (CyA, 0.5 μM). Subsequently, cells were exposed to thapsigargin (TG, 1.5 μM) for 1 h followed by a 6-h exposure to hydrogen peroxide (H_2O_2, 100 μM). (C) Rat1a fibroblasts were pretreated with ROS inhibitors MnTBAP (50 μM) and NAC (1 mM) and exposed to 0% O_2 for 48 h. (D) HT1080 fibrosarcoma cells transfected with a control vector or with MnSOD and catalase targeted to the mitochondria (HT1080-MnSOD/mCAT) for 0% O_2 for 48 h. *, $P < 0.05$ compared with cells exposed to 21% O_2.

chondria and used by the F_1F_0-ATP synthase to generate a ψ. Indeed, two different F_1F_0-ATP synthase inhibitors, oligomycin and aurovertin B, diminished the ψ of Bcl-X_L cells during oxygen deprivation (Fig. 7B). Consistent with these findings, the glycolytic inhibitor 2-DOG and the adenine nucleotide translocator (ANT) inhibitor atractyloside diminished the ψ of Bcl-X_L cells during oxygen deprivation. Furthermore, Bcl-X_L failed to prevent oxygen deprivation-induced cell death in the presence of oligomycin, aurovertin B, and atractyloside (Fig. 7C). Oligomycin, aurovertin B, atractyloside, and 2-DOG all independently induced cell death under normal oxygen conditions in Neo control cells but not in Bcl-X_L cells (data not shown). Hence, the ability of Bcl-X_L to prevent oxygen deprivation-induced cell death depends on the ability of the F_1F_0-ATP synthase to utilize glycolytic ATP to generate a ψ.

DISCUSSION

Apoptosis and necrosis are defined as two distinct forms of cell death that can be distinguished based on cellular morphology (20). Apoptotic cells display intranucleosomal DNA cleavage and shrink while neighboring cells rapidly engulf them. In contrast, necrotic cells tend to swell and burst, resulting in the spilling of their intracellular contents over neighboring cells, which triggers an inflammatory response. Tissues in vivo exposed to conditions of oxygen deprivation due to an occlusion of a blood vessel simultaneously contain cells that have undergone apoptosis and those that have undergone necrosis (17). In the present study we investigated whether fibroblasts in vitro undergo apoptosis or necrosis during oxygen deprivation. We found that Rat1a fibroblasts undergo apoptosis during oxygen deprivation and undergo necrosis only if they are deprived of oxygen and glucose simultaneously. Cell death during oxygen deprivation is associated with DNA fragmentation and apoptotic nuclei and is preceded by the release of cytochrome *c* from mitochondria and activation of caspase-9. The commitment to death in cells deprived of oxygen occurred at the point when cells released cytochrome *c* and activated caspase-9. The antiapoptotic protein Bcl-X_L prevented the release of cytochrome *c*, activation of caspase-9, and cell death in response to

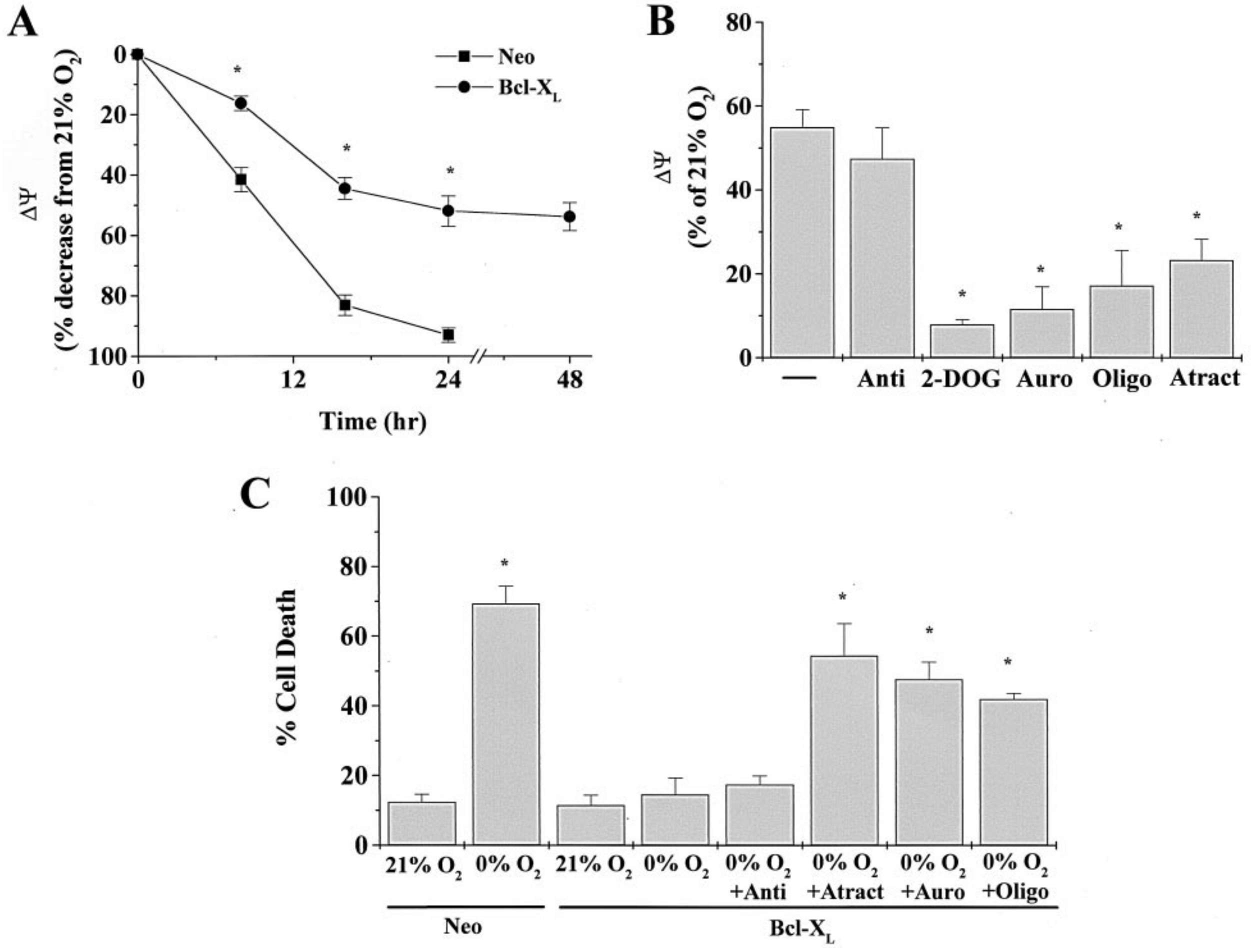

FIG. 7. Bcl-X_L prevents cell death by allowing glycolytic ATP to maintain a partial mitochondrial membrane potential via the F_1F_0-ATP synthase. (A) Neo and Bcl-X_L-transfected cells were exposed to 0% O_2 for 8, 16, 24, and 48 h, and the mitochondrial membrane potential (ψ) was measured as described in Materials and Methods. A large fraction of Neo cells at 48 h were dead; therefore, ψ was not measured. $*$, $P < 0.05$ for Bcl-X_L cells compared with Neo cells. (B) Bcl-X_L cells were exposed to 0% O_2 for 22 h and subsequently incubated with the fluorescence probes TMRE and MITO for 2 h at 0% O_2 in the presence of antimycin a (Anti, 1 μg/ml), 2-DOG (12 mM), aurovertin B (Auro, 30 μM), oligomycin (Oligo, 1 μg/ml), and atractyloside (Atract, 1 mM). $*$, $P < 0.05$ compared with Bcl-X_L cells exposed to 0% O_2. (C) Bcl-X_L cells were exposed to 0% O_2 for 48 h in the presence of antimycin a (Anti, 1 μg/ml), atractyloside (Atract, 1 mM), aurovertin B (Auro, 30 μM), and oligomycin (Oligo, 1 μg/ml) and assayed for LDH release. $*$, $P < 0.05$ compared with Neo control cells exposed to 21% O_2.

oxygen deprivation. The broad-based caspase inhibitor zVAD-fmk did not inhibit the release of cytochrome *c*, indicative of a caspase-independent mechanism of cytochrome *c* release. The apoptotic cell death observed during oxygen deprivation was not accompanied by a significant activation of caspase-8. Rat1a fibroblasts typically are refractory to CD95-mediated cell death unless the oncogene Myc is active in these cells (11). Therefore, the extrinsic apoptotic pathway is likely not an important regulator of cell death in Rat1a fibroblasts during oxygen deprivation. These results indicate that cells undergoing oxygen deprivation die through an intrinsic apoptotic pathway.

Bcl-X_L did not prevent the release of cytochrome *c* or cell death in cells deprived of oxygen and glucose. Cells deprived of oxygen and glucose also did not display caspase-9 activation, DNA fragmentation, or apoptotic nuclei indicative of necrosis under these conditions. Since cytochrome *c* release from mitochondria into the cytosol typically accompanies the activation of caspase-9 in the presence of ATP, we examined the energetic status of cells deprived of oxygen and glucose. Cells deprived of oxygen and glucose displayed a complete loss of cellular ATP levels, while cells deprived of oxygen alone exhibited a partial maintenance of ATP levels compared with cells under normal oxygen conditions. Thus, the necrotic morphology observed during oxygen and glucose deprivation is due to the lack of ATP available to trigger activation of caspase-9.

Deprivation of growth factors is one of the best-described death stimuli that utilize the intrinsic apoptotic pathway. The activation of PI3K and its downstream effector, the serine/threonine kinase Akt, is a major mechanism by which growth factors promote cell survival (18). Previous studies have shown that Akt can confer a survival signal in Rat1a fibroblasts in the absence of serum (19). However, our present results show that Rat1a fibroblasts that contain an activated form of Akt are still sensitive to oxygen deprivation, indicating that the pathways regulating serum and oxygen deprivation diverge. Recent work has demonstrated that both Akt and Bcl-2/Bcl-X_L inhibit apoptosis by maintaining mitochondrial integrity (7, 36). However, unlike Bcl-2/Bcl-X_L, the ability of Akt to inhibit apoptosis and cytochrome *c* release is dependent upon the availability of glucose and on the coupling of oxidative phosphorylation and glycolysis via mitochondrial hexokinase (7). Thus, it is likely that Akt cannot inhibit oxygen deprivation-induced cell death because of uncoupling of oxidative phosphorylation and glycolysis.

Recently, it has been postulated that PI3K plays an important role in angiogenesis and regulates VEGF expression (13, 32). Cells expressing activated PI3K or Akt display an increase in levels of VEGF mRNA under normal oxygen conditions. Cells that typically encounter conditions of low oxygen levels (1 to 3% O_2) in vivo activate angiogenesis through the release of factors such as VEGF. Angiogenesis would provide more oxygen and nutrients and prevent cells from reaching the 0% O_2 condition, which will trigger apoptosis. Therefore, Akt-induced angiogenesis might prevent cellular oxygen deprivation in tissues. In the present study, an activated form of Akt in Rat1a fibroblasts was able to stimulate release of VEGF under normoxic conditions similar to levels found under hypoxic conditions in cells that do not contain an activated Akt. Bcl-X_L had no effect on the release of VEGF under normoxic or hypoxic conditions.

DNA damage due to gamma irradiation is another stimulus that utilizes the intrinsic apoptotic pathway (27). DNA-damaging agents utilize a p53-dependent apoptotic pathway in many cell types (3, 29). Oxygen deprivation has been shown to induce p53 protein accumulation and p53-dependent apoptosis in oncogenically transformed cells (8, 40). It has been postulated that mutations in p53 may promote tumor cell growth and survival by allowing cells to avoid oxygen deprivation-induced apoptosis. Our present observations indicate that $p53^{-/-}$ MEFs are able to undergo cell death under oxygen deprivation. These results suggest that the role of p53 in regulating oxygen deprivation-induced cell death may be restricted to oncogenically transformed cells.

A common element in the intrinsic apoptotic pathway induced by deprivation of growth factors or DNA damage is the requirement of Bax or Bak (51). Cells from mice with double knockouts of these proapoptotic Bcl-2 family members are resistant to apoptosis from gamma irradiation and serum deprivation. In contrast, neither Bax nor Bak was required for Fas-mediated death. In the present study we observed that MEFs lacking Bax and Bak were resistant to oxygen deprivation, indicating that Bax or Bak is required for oxygen deprivation-induced cell death. Taken together, the observations that Bcl-X_L and the loss of Bax or Bak prevent oxygen deprivation-induced apoptosis indicate that the Bcl-2 family members regulate the oxygen deprivation apoptotic pathway.

What might initiate the apoptotic cascade in cells exposed to oxygen deprivation? Cell survival depends on the oxidation of NADH coupled to the reduction of oxygen to generate ATP by the F_1F_0-ATP synthase. Oxygen is reduced to water by cytochrome *c* oxidase. A lack of oxygen would inhibit the electron transport chain at cytochrome *c* oxidase, resulting in the initiation of a death cascade through Bax or Bak. Consistent with this hypothesis is the observation that ρ° fibroblasts do not undergo cell death in response to oxygen deprivation. The mitochondrial DNA encodes for 13 polypeptides, including subunits for cytochrome *c* oxidase. Therefore, ρ° cells do not have a functional electron transport chain and rely on glycolytic ATP for their energetic needs (1). The cell death pathway is intact in ρ° cells, as shown by their ability to undergo death in response to doxorubicin. It is possible that these cells in the process of generation might have gained a selective advantage that renders them resistance to oxygen deprivation. However, we generated multiple different populations of ρ° cells, all of which were resistant to oxygen deprivation but remained sensitive to doxorubicin. Moreover, previous studies have demonstrated that ρ° cells die in response to growth factor withdrawal (12). It is likely that during growth factor withdrawal or doxorubicin treatment, ρ° cells retain signals that regulate Bax or Bak to induce cell death. In contrast, a lack of functional electron transport does not allow ρ° cells during oxygen deprivation to initiate signals that would regulate Bax or Bak to induce cell death. These data suggest that inhibition of electron transport chain is an upstream event from Bax or Bak in the oxygen deprivation induction of the intrinsic apoptotic pathway.

The ability of Bcl-X_L to prevent cytochrome *c* release during oxygen deprivation suggests that the permeability of the outer mitochondrial membrane is an important regulatory target during oxygen deprivation-induced cell death. Currently, there are two models to explain the release of cytochrome *c* (31). The first model evokes the formation of large channels by proapoptotic Bcl-2 family members in the outer mitochondrial membrane sufficient to transport cytochrome *c*. Further, Bcl-X_L can bind to the proapoptotic Bcl-2 family members to prevent the formation of these channels. The second model suggests a nonspecific rupture of the outer mitochondrial membrane by mitochondrial matrix swelling. Mitochondrial swelling has been reported to occur in response to many apoptotic stimuli, including growth factor withdrawal and oxygen deprivation (10, 48). One mechanism proposed to cause matrix swelling is the formation of the PTP (23). The PTP is a large-conductance channel proposed to span both mitochondrial membranes. Opening of the pore is characterized by an abrupt increase in the permeability of the inner mitochondrial membrane to molecules as large as 1,500 Da. Primary evidence for the PTP model comes from experiments showing that cyclosporine and trifluoperazine, inhibitors of PTP formation, prevent cell death. However, our data indicate that neither cyclosporine nor trifluoperazine prevents cell death in response to oxygen deprivation in Rat1a fibroblasts. Thus, the PTP may not be a regulator of oxygen deprivation-induced cell death.

Another mechanism that can cause swelling of the mitochondrial matrix, resulting in outer mitochondrial membrane rupture, is the closure of the voltage-dependent anion channel (VDAC) observed in cells undergoing apoptosis in response to growth factor deprivation (45, 46). Under normal physiologic conditions, electron transfer through the respiratory chain is coupled to the directional movement of protons across the inner mitochondrial membrane. This movement across the membrane establishes a pH gradient and a membrane potential that provides the thermodynamic driving force for F_1F_0-ATP synthase to generate ATP in the matrix. Cytosolic ADP must be transported across both the inner and the outer mitochondrial membranes for the F_1F_0-ATP synthase to generate ATP. The principal mediators of ATP/ADP exchange are ANT on the inner mitochondrial membrane and VDAC on the outer mitochondrial membrane. The closure of VDAC results in the impairment of the exchange of cytosolic ADP for mitochondrial ATP. The defect in exchange causes the hyperpolarization of the inner mitochondrial membrane by limiting the ability of ATP synthase to utilize the potential to generate ATP from ADP. Subsequently, the electron transport chain slows and the matrix swells. Bcl-X_L can prevent the closure of VDAC and allow the efficient exchange of cytosolic ADP for mitochondrial ATP. During oxygen deprivation, the electron transport chain ceases and a hydrogen ion gradient does not develop. Subsequently, the F_1F_0-ATP synthase does not generate ATP. Under these conditions, the F_1F_0-ATP synthase has the capacity to hydrolyze glycolytic ATP and extrude protons from the matrix in an attempt to maintain mitochondrial membrane potential (34). However, Rat1a fibroblasts displayed a continuous decrease in mitochondrial membrane potential prior to cytochrome *c* release, suggesting that the F_1F_0-ATP synthase was not efficient in maintaining the potential. In contrast, Rat1a fibroblasts that overexpress Bcl-X_L were able to maintain a potential, and inhibitors of the F_1F_0-ATP synthase, ANT, and glycolysis independently dissipated the potential. Furthermore, all three inhibitors abolished the ability of Bcl-X_L to prevent cell death during oxygen deprivation. These results suggest that Bcl-X_L prevents cell death by allowing glycolytic ATP to be utilized by the F_1F_0-ATP synthase in order to maintain a mitochondrial membrane potential. Since ATP fell to similar levels in both control and Bcl-X_L cells during oxygen deprivation, this suggests that Bcl-X_L does not regulate glycolytic ATP production during oxygen deprivation. Thus, Bcl-X_L either regulates the efficient exchange of glycolytic ATP across the inner and outer mitochondrial membranes or affects the ability of the F_1F_0-ATP synthase to utilize glycolytic ATP. The localization of Bcl-2 family members on the outer membrane, however, suggests that Bcl-X_L may allow efficient exchange of glycolytic ATP across VDAC to maintain a potential and the subsequent survival of cells during oxygen deprivation.

In summary, the present data indicate a requirement for a functional electron transport chain and the proapoptotic Bcl-2 family members Bax or Bak for oxygen deprivation-induced cell death. The antiapoptotic Bcl-2 family member Bcl-X_L might prevent oxygen deprivation-induced cell death by allowing glycolytic ATP to be used by the F_1F_0-ATP synthase in order to maintain a mitochondrial membrane potential and cell survival. Taken together, these results suggest that components of both the inner and outer mitochondrial membranes serve as important regulators of oxygen deprivation-induced cell death.

ACKNOWLEDGMENT

This work was supported by grant GM60472-02 from the National Institutes of Health to N.S.C.

REFERENCES

1. **Buchet, K., and C. Godinot.** 1998. Functional F1-ATPase essential in maintaining growth and membrane potential of human mitochondrial DNA-depleted ρ° cells. J. Biol. Chem. **273:**22983–22989.
2. **Byun, Y., F., Chen, R. Chang, M. Trivedi, K. J. Green, and V. L. Cryns.** 2001. Caspase cleavage of vimentin disrupts intermediate filaments and promotes apoptosis. Cell Death Differ. **8:**443–450.
3. **Clarke, A. R., C. A. Purdie, D. J. Harrison, R. G. Morris, C. C. Bird, M. L. Hooper, and A. H. Wyllie.** 1993. Thymocyte apoptosis induced by p53-dependent and independent pathways. Nature **362:**849–852.
4. **Datta, S. R., A. Brunet, and M. E. Greenberg.** 1999. Cellular survival: a play in three Akts. Genes Dev. **13:**2905–2927.
5. **Degli Esposti, M., and H. McLennan.** 1998. Mitochondria and cells produce reactive oxygen species in virtual anaerobiosis: relevance to ceramide-induced apoptosis. FEBS Lett. **430:**338–342.
6. **Formigli, L., L. Papucci, A. Tani, N. Schiavone, A. Tempestini, G. E. Orlandini, S. Capaccioli, and S. Z. Orlandini.** 2000. Aponecrosis: morphological and biochemical exploration of a syncretic process of cell death sharing apoptosis and necrosis. J. Cell Physiol. **182:**41–49.
7. **Gottlob, K., S. Kennedy, E. Kandel, R. B. Robey, and N. Hay.** 2001. Inhibition of early apoptotic events by Akt/PKB is dependent on the first committed step of glycolysis and mitochondrial hexokinase. Genes Dev. **15:**1406–1418.
8. **Graeber, T. G., C. Osmanian, T. Jacks, D. E. Housman, C. J. Koch, S. W. Lowe, and A. J. Giaccia.** 1996. Hypoxia-mediated selection of cells with diminished apoptotic potential in solid tumours. Nature **379:**88–91.
9. **Green, D. R.** 2000. Apoptotic pathways: paper wraps stone blunts scissors. Cell **102:**1–4.
10. **Heffner, R. R., and S. A. Barron.** 1978. The early effects of ischemia upon skeletal muscle mitochondria. J. Neurol. Sci. **38:**295–315.
11. **Hueber, A. O., M. Zornig, D. Lyon, T. Suda, S. Nagata, and G. I. Evan.** 1997. Requirement for the CD95 receptor-ligand pathway in c-Myc-induced apoptosis. Science **278:**1305–1309.
12. **Jacobson, M. D., J. F. Burne, M. P. King, T. Miyashita, J. C. Reed, and M. C. Raff.** 1993. Bcl-2 blocks apoptosis in cells lacking mitochondrial DNA. Nature **361:**365–369.
13. **Jiang, B. H., J. Z. Zheng, M. Aoki, and P. K. Vogt.** 2000. Phosphatidylinositol 3-kinase signaling mediates angiogenesis and expression of vascular endothelial growth factor in endothelial cells. Proc. Natl. Acad. Sci. USA **97:**1749–1753.
14. **Jurgensmeier, J. M., Z. Xie, Q. Deveraux, L. Ellerby, D. Bredesen, and J. C. Reed.** 1998. Bax directly induces release of cytochrome *c* from isolated mitochondria. Proc. Natl. Acad. Sci. USA **95:**4997–5002.
15. **Kandel, E. S., and N. Hay.** 1999. The regulation and activities of the multifunctional serine/threonine kinase Akt/PKB. Exp. Cell Res. **253:**210–229.
16. **Kang, P. M., and S. Izumo.** 2000. Apoptosis and heart failure: a critical review of the literature. Circ. Res. **86:**1107–1113.
17. **Kang, P. M., A. Haunstetter, H. Aoki, A. Usheva, and S. Izumo.** 2000. Morphological and molecular characterization of adult cardiomyocyte apoptosis during hypoxia and reoxygenation. Circ. Res. **87:**118–125.
18. **Kennedy, S. G., A. J. Wagner, S. D. Conzen, J. Jordan, A. Bellacosa, P. N. Tsichlis, and N. Hay.** 1997. The PI 3-kinase/Akt signaling pathway delivers an anti-apoptotic signal. Genes Dev. **11:**701–713.
19. **Kennedy, S. G., E. S. Kandel, T. K. Cross, and N. Hay.** 1999. Akt/protein kinase B inhibits cell death by preventing the release of cytochrome *c* from mitochondria. Mol. Cell. Biol. **19:**5800–5810.
20. **Kerr, J. F., A. H. Wyllie, and A. R. Currie.** 1972. Apoptosis: a basic biological phenomenon with wide-ranging implications in tissue kinetics. Br. J. Cancer **26:**239–257.
21. **Kluck, R. M., E. Bossy-Wetzel, D. R. Green, and D. D. Newmeyer.** 1997. The release of cytochrome *c* from mitochondria: a primary site for Bcl-2 regulation of apoptosis. Science **275:**1132–1136.
22. **Kluck, R. M., M. D. Esposti, G. Perkins, C. Renken, T. Kuwana, E. Bossy-Wetzel, M. Goldberg, T. Allen, M. J. Barber, D. R. Green, and D. D. Newmeyer.** 1999. The pro-apoptotic proteins, Bid and Bax, cause a limited permeabilization of the mitochondrial outer membrane that is enhanced by cytosol. J. Cell Biol. **147:**809–822.
23. **Kroemer, G., and J. C. Reed.** 2000. Mitochondrial control of cell death. Nat. Med. **6:**513–519.
24. **Lemasters, J. J., A. L. Nieminen, T. Qian, L. C. Trost, and B. Herman.** 1997. The mitochondrial permeability transition in toxic, hypoxic and reperfusion injury. Mol. Cell. Biochem. **174:**159–165.
25. **Li, H., H. Zhu, C. J. Xu, and J. Yuan.** 1998. Cleavage of BID by caspase-8 mediates the mitochondrial damage in the Fas pathway of apoptosis. Cell **94:**491–501.
26. **Li, P., D. Nijhawan, I. Budihardjo, S. M. Srinivasula, M. Ahmad, E. S. Alnemri, and X. Wang.** 1997. Cytochrome *c* and dATP-dependent formation of Apaf-1/caspase-9 complex initiates an apoptotic protease cascade. Cell **91:**479–489.
27. **Lindsten, T., A. J. Ross, A. King, W. X. Zong, J. C. Rathmell, H. A. Shiels, E. Ulrich, K. G. Waymire, P. Mahar, K. Frauwirth, Y. Chen, M. Wei, V. M. Eng, D. M. Adelman, M. C. Simon, A. Ma, J. A. Golden, G. Evan, S. J. Korsmeyer, G. R. MacGregor, and C. B. Thompson.** 2000. The combined functions of proapoptotic Bcl-2 family members Bax and Bak are essential for normal development of multiple tissues. Mol. Cell **6:**1389–1399.
28. **Liu, X., C. N. Kim, J. Yang, R. Jemmerson, and X. Wang.** 1996. Induction of apoptotic program in cell-free extracts: requirement for dATP and cytochrome *c*. Cell **86:**147–157.
29. **Lowe, S. W., E. M. Schmitt, S. W. Smith, B. A. Osborne, and T. Jacks.** 1993.

p53 is required for radiation-induced apoptosis in mouse thymocytes. Nature **362:**847–849.

30. **Luo, X., I. Budihardjo, H. Zou, C. Slaughter, and X. Wang.** 1998. Bid, a Bcl2 interacting protein, mediates cytochrome *c* release from mitochondria in response to activation of cell surface death receptors. Cell **94:**481–490.
31. **Martinou, J. C., and D. R. Green.** 2001. Breaking the mitochondrial barrier. Nat. Rev. Mol. Cell. Biol. **2:**63–67.
32. **Mazure, N. M., E. Y. Chen, K. R. Laderoute, and A. M. Giaccia.** 1997. Induction of vascular endothelial growth factor by hypoxia is modulated by a phosphatidylinositol 3-kinase/Akt signaling pathway in Ha-ras-transformed cells through a hypoxia inducible factor-1 transcriptional element. Blood **90:**3322–3331.
33. **Nagata, S.** 1997. Apoptosis by death factor. Cell **88:**355–365.
34. **Nicholls, D. G.** 1974. The influence of respiration and ATP hydrolysis on the proton-electrochemical gradient across the inner membrane of rat-liver mitochondria as determined by ion distribution. Eur. J. Biochem. **50:**305–315.
35. **Peter, M. E., and P. H. Krammer.** 1998. Mechanisms of CD95 (APO-1/Fas)-mediated apoptosis. Curr. Opin. Immunol. **10:**545–551.
36. **Plas, D. R., S. Talapatra, A. L. Edinger, J. C. Rathmell, and C. B. Thompson.** 2001. Akt and Bcl-X_L promote growth factor-independent survival through distinct effects on mitochondrial physiology. J. Biol. Chem. **276:**12041–12048.
37. **Rodriguez, A. M., P. M. Carrico, J. E. Mazurkiewicz, and J. A. Melendez.** 2000. Mitochondrial or cytosolic catalase reverses the MnSOD-dependent inhibition of proliferation by enhancing respiratory chain activity, net ATP production, and decreasing the steady state levels of H_2O_2. Free Radic. Biol. Med. **29:**801–813.
38. **Saikumar, P., Z. Dong, Y. Patel, K. Hall, U. Hopfer, J. M. Weinberg, and M. A. Venkatachalam.** 1998. Role of hypoxia-induced Bax translocation and cytochrome *c* release in reoxygenation injury. Oncogene **17:**3401–3415.
39. **Saikumar, P., Z. Dong, J. M. Weinberg, and M. A. Venkatachalam.** 1998. Mechanisms of cell death in hypoxia/reoxygenation injury. Oncogene **17:**3341–3349.
40. **Schmaltz, C., P. H. Hardenbergh, A. Wells, and D. E. Fisher.** 1998. Regulation of proliferation-survival decisions during tumor cell hypoxia. Mol. Cell. Biol. **18:**2845–2854.
41. **Shimizu, S., Y. Eguchi, H. Kosaka, W. Kamiike, H. Matsuda, and Y. Tsujimoto.** 1995. Prevention of hypoxia-induced cell death by Bcl-2 and Bcl-X_L. Nature **374:**811–813.
42. **Strasser, A., A. W. Harris, D. C. S. Huang, P. H. Krammer, and S. Cory.** 1995. Bcl-2 and Fas/APO-1 regulate distinct pathways to lymphocyte apoptosis. EMBO J. **14:**6136–6147.
43. **Tamatani, M., T. Matsuyama, A. Yamaguchi, N. Mitsuda, Y. Tsukamoto, M. Taniguchi, Y. H. Che, K. Ozawa, O. Hori, H. Nishimura, A. Yamashita, M. Okabe, H. Yanagi, D. M. Stern, S. Ogawa, and M. Tohyama.** 2001. ORP150 protects against hypoxia/ischemia-induced neuronal death. Nat. Med. **7:**317–323.
44. **Thompson, C. B.** 1995. Apoptosis in the pathogenesis and treatment of disease. Science **267:**1456–1462.
45. **Vander Heiden, M. G., X. X. Li, E. Gottleib, R. B. Hill, C. B. Thompson, and M. Colombini.** 2001. Bcl-xL promotes the open configuration of the voltage-dependent anion channel and metabolite passage through the outer mitochondrial membrane. J. Biol. Chem. **276:**19414–19419.
46. **Vander Heiden, M. G., N. S. Chandel, X. X. Li, P. T. Schumacker, M. Colombini, and C. B. Thompson.** 2000. Outer mitochondrial membrane permeability can regulate coupled respiration and cell survival. Proc. Natl. Acad. Sci. USA **97:**4666–4671.
47. **Vander Heiden, M. G., N. S. Chandel, P. T. Schumacker, and C. B. Thompson.** 1999. Bcl-X_L prevents cell death following growth factor withdrawal by facilitating mitochondrial ATP/ADP exchange. Mol. Cell **3:**159–167.
48. **Vander Heiden, M. G., N. S. Chandel, E. K. Williamson, P. T. Schumacker, and C. B. Thompson.** 1997. Bcl-X_L regulates the membrane potential and volume homeostasis of mitochondria. Cell **91:**627–637.
49. **Vaux, D. L., and S. J. Korsmeyer.** 1999. Cell death in development. Cell **96:**245–254.
50. **Wei, M. C., T. Lindsten, V. K. Mootha, S. Weiler, A. Gross, M. Ashiya, C. B. Thompson, and S. J. Korsmeyer.** 2000. tBID, a membrane-targeted death ligand, oligomerizes BAK to release cytochrome *c*. Genes Dev. **14:**2060–2071.
51. **Wei, M. C., W. X. Zong, E. H. Y. Cheng, T. Lindsten, V. Panoutsakopoulou, A. J. Ross, K. A. Roth, G. R. MacGregor, C. B. Thompson, and S. J. Korsmeyer.** 2001. Pro-apoptotic BAX and BAK are a requisite gateway to mitochondrial dysfunction and death. Science **292:**727–730.
52. **Yang, J., X. Liu, K. Bhalla, C. N. Kim, A. M. Ibrado, J. Cai, T. I. Peng, D. P. Jones, and X. Wang.** 1997. Prevention of apoptosis by Bcl-2: release of cytochrome *c* from mitochondria blocked. Science **275:**1129–1132.